Water driven Flow of Carbon Nanotubes in a Rotating Channel

Article *in* Journal of Molecular Liquids · November 2015

DOI: 10.1016/j.molliq.2015.11.042

4 authors:

Syed Tayyab Hussain
National University of Sciences and Technology
12 PUBLICATIONS **163** CITATIONS
SEE PROFILE

Rizwan Ul Haq
Bahria University Islamabad Campus
77 PUBLICATIONS **1,350** CITATIONS
SEE PROFILE

Zafar Hayat Khan
University of Malakand
85 PUBLICATIONS **1,672** CITATIONS
SEE PROFILE

Prof. Dr. Sohail Nadeem
Quaid-i-Azam University
388 PUBLICATIONS **7,121** CITATIONS
SEE PROFILE

Journal of Molecular Liquids 214 (2016) 136–144

Contents lists available at ScienceDirect

Journal of Molecular Liquids

journal homepage: www.elsevier.com/locate/molliq

Water driven flow of carbon nanotubes in a rotating channel

S.T. Hussain [a], Rizwan-ul- Haq [b,*], Z.H. Khan [c], S. Nadeem [a]

[a] Department of Mathematics, Quaid-i-Azam University, Islamabad 44000, Pakistan
[b] Department of Mathematics, Capital University of Science and Technology (CUST), Islamabad, Pakistan
[c] Department of Mathematics, University of Malakand, Dir (Lower), Khyber Pakhtunkhwa, Pakistan

ARTICLE INFO

Article history:
Received 10 September 2015
Received in revised form 11 November 2015
Accepted 19 November 2015
Available online xxxx

Keywords:
Nanofluid flow
Rotating channel
Single wall carbon nanotube
Multiple wall carbon nanotube

ABSTRACT

In this article, flow and heat transfer effects of both single and multiple wall carbon nanotubes within the base fluid (water) are analyzed between two rotating plates. Moreover, we have considered that the upper wall of the channel is permeable while the lower wall is moving with variable velocity to produce the forced convection along with the Coriolis and centripetal forces with the rotation of fluid. The compatible transformations have been used to construct the non-dimensional system of governing equations. Numerical simulation is performed to obtain the solutions structure. Thermophysical properties of each base fluid and nano particle are incorporated in the form of thermal conductivity, viscosity, density, specific heat, nanoparticle volume fraction and Prandtl number to attain the solution of the model. It is found that water based single wall carbon nanotubes (SWCNTs) produce less drag and high heat transfer rate as compared to the water based multiple wall carbon nanotubes (MWCNTs). Influence of rotation causes the drag increase and decreases the Nusselt number irrespective of the other pertinent parameters. Moreover suction/injection plays an important role in determining the peak position of velocity. The effect of suction/injection is shown through plotting streamlines.

1. Introduction

Fluid flow and heat transfer in a channel is one of the most important phenomena in high performance heat exchangers, chemical reactors, nuclear power plants, high temperature boiling plants, petroleum refineries and refrigeration process. During these processes the basic principle is to efficiently manage the heat transfer process and reduce the drag. Flows in rotating machines are modeled by using the rotating frame of references. Rotating flows have numerous applications in applications in turbomachinery. Rotating frames are not physically rotating anything and therefore transient effects are not visible due to the real motion. The rotating frame of reference approach can be used to solve the problems where transient effects due to rotor–stator interaction are small. A typical example is the mixing tank where the impeller–baffle interactions are relatively weak; large-scale transient effects are not present. The energy transfer between the fluid and rotor is an important feature in several rotating machines. Therefore, the study of rotating flows in the presence of nanoparticles will explore the possibility of heat transfer enhancement.

In heat transfer studies one field which has gained immense interest from the researchers is nanofluid flow. Nanofluids are a of base fluid and nanoparticles. Nanoparticles can be metallic (Cu, Zn, Al, etc.) or non-metallic and even chain of particles (carbon nanotubes). Nanofluids have considerable advantages over the ordinary fluids due to the enhanced thermal conductivity. Initially, Choi [1] introduced the concept of nanofluid based on incorporation of nano sized (10^{-9} to 10^{-11} nm) particles in a fluid. Masuda et al. [2] showed the thermal conductivity enhancement due to addition of ultra-fine sized particles, which were called nanoparticles. After Masuda [2], Pak and Cho [3] discussed the heat transfer due to addition of submicron metallic oxide particles in the base fluid. Their study concluded that the alteration in heat transfer rate was mainly due to higher thermal conductivity of submicron particles. Recently, several studies [4–6] were published on the analysis of heat transfer due to incorporation of nanoparticles in base fluid. Boungiorno [7] developed a mathematical model to study nanofluid flow. Seven slip phenomena were considered which can be important and proved that only Brownian motion and Thermophoresis are the dominant ones in relevance to nano fluids. This model hasn't taken into account the effect of shapes of nanoparticles in heat transfer. Recent studies [8–10] have showed that shape of and nature of nanoparticles are important factors to enhance the thermal conductivity of working fluid. Effect of shape on heat transfer has been examined by Elias et al. [11], they considered five different shape nanoparticles (cylindrical, spherical, bricks, blades and platelets). Their study showed that although all of them increase the heat transfer characteristics yet cylindrical shape nanoparticles have higher heat transfer rate. Vanaki et al. [12] discussed the effect of turbulent nanofluid flow in a wavy channel under different shaped SiO_2 nanoparticles. They concluded that platelet shape particles have better performance in heat transfer phenomenon. Jeong et al. [13] showed that particle shape has significant effect on the viscosity and thermal conductivity of base

* Corresponding author.
E-mail addresses: ideal_riz@hotmail.com, r.haq.qau@gmail.com (R.- Haq).

http://dx.doi.org/10.1016/j.molliq.2015.11.042
0167-7322/

fluid. They found that rectangular shaped particles increased the viscosity of base fluid by 69% and it is 7.7% higher than that of the spherical shape particles. Timofeeva et al. [14] experimentally showed that shape of the nanoparticle played an important role in percentage increase in the thermal conductivity of base fluid and blade shaped nanoparticles have higher thermal conductivity compared to the rest of shapes.

Carbon nanotubes (CNTs) are cylindrical shapes like structures of carbon atoms with diameter ranges between 1 and 50 nm. They exhibit exceptional electrical, mechanical, thermal and optical properties at individual level. According to the details given by the CNT manufacturing firm NTI, at individual tube level CNT particles have; two hundred times strength and five times elasticity of steel, fifteen times thermal conductivity and thousand times the current capacity of copper and half the density of aluminum. Moreover CNTs don't possess any threat to the environment due to presences of carbon chains. Thus Environmental Protection Agency (EPA) declared them articles which are not hazardous or toxic for the environment. Hence, it is important to explore the effects of CNT on the fluid flow and heat transfer of Newtonian and non-Newtonian fluids. Haq et al. [15] considered the water based flow in the presence of single wall carbon nanotubes (SWCNTs) and multiple wall carbon nanotubes (MWCNTs). Their study reported the higher Nusselt number and skin friction for SWCNT than the MWCNT. In another study Haq et al. [16] showed that engine oil based CNT fluid has higher skin friction and heat transfer rate as compared to water and kerosene based CNT fluid.

Stretching is an important phenomenon in the production of polymer sheets, drawing of copper wires and film coatings. Sakiadis [17] pioneered the idea of boundary layer flow over a continuously moving surface and modeled the two-dimensional boundary layer equations. Tsou et al. [18] extended this work to examine the effects of stretching sheet on the momentum and heat transfer. Erickson et al. [19] took it further to examine the effect of mass transfer by considering suction/injection at the wall. Nadeem and Hussain [20] discussed the flow of Williamson nanofluid over a linearly stretching surface. It has been showed that Lewis number appearance in the governing equations depends upon what types of similarity transformations have been chosen. In another article, Hussain et al. [21] discussed the micro-rotation effect on the nanofluid flow over a linearly stretching surface. It has been showed that micro-rotation has a decreasing effect on skin friction while an increasing effect on heat transfer rate. In recent years, several studies [22–30] have been reported on the boundary layer flow of a nanofluid over a continuously moving surface. But only few articles have been written considering the nanofluid flow in a channel with the stretching of lower plate along the axis of flow. Borakati and Bharali [31] examined the effect of magnetic field on the two-dimensional channel flows with heat transfer in a rotating system. Hussnain et al. [32] obtained the HAM solution for three-dimensional flow of second grade in a rotating frame. Large values of rotation parameter caused the reversal of flow and fully develop flow is achieved with the increasing values of suction/injection parameter. Vajravelu and Kumar [33] presented the analytic and numerical solution for the two-dimensional flow in a channel and discussed the effect of rotation parameter on the velocity. Freidoonimehr [34] discussed the effects of different nanoparticles on the velocity and skin friction of the water based fluid in the rotating channel. Recently, Sheikholeslami et al. [35] discussed the Cu–water nanofluid flow between a porous plate and a stretching surface in a rotating system. Their study reported that the skin friction coefficient and the Nusselt number are greatly influenced by the presence of nanoparticles. Moreover the coefficient of skin friction and Nusselt number decreases with the increase in rotation parameter. Recent studies attain the considerable attention at industrial level and daily usage lubricant to transfer, remove or add the heat based on thermal conductivity [36–40].

The aim of the present article is to discuss the effects of single and multiple wall carbon nanotubes on the fluid flow and heat transfer of water based fluid in a rotating frame of reference where the lower plate is continuously moving along the horizontal axis and the upper plate is porous. Thermo-physical properties of SWCNTs, MWCNTs, Prandtl number and densities are used to develop the steady state solutions. Flow field results are discussed through plotting the graphs of velocity and temperature profile. Moreover the drag and heat transfer rate are examined by plotting the graphs of skin friction coefficient and Nusselt number against the nanoparticle volumetric fraction and pertinent parameters. To the best of the authors' knowledge no study reports the effect of CNTs on the fluid flow and heat transfer in the rotating channel.

2. Mathematical modeling

Let us consider an incompressible flow of water based CNTs confined between two infinite plates in a rotating frame of reference (angular velocity $\boldsymbol{\Omega}[0,\Omega,0]$). The upper plate is porous and the lower plate is moving with velocity $U_w = ax$ ($a>0$). The steady state velocity field is defined as $\boldsymbol{V}[u(x,y),v(x,y),w(x,y)]$, where u, v, w are the velocity components along x, y and z direction, respectively. The schematic diagram of the problem is shown in Fig. 1:

The momentum governing equation for rotating flow is

$$\rho_{nf}\left(\frac{d\boldsymbol{V}}{dt}+2\boldsymbol{\Omega}\times\boldsymbol{V}+\boldsymbol{\Omega}\times(\boldsymbol{\Omega}\times\mathbf{r})\right)=div\boldsymbol{T}. \tag{1}$$

$2\boldsymbol{\Omega}\times\boldsymbol{V}$ is the Coriolis force whose direction is perpendicular to both $\boldsymbol{\Omega}$ and $\boldsymbol{V}$. $\boldsymbol{\Omega}\times(\boldsymbol{\Omega}\times\boldsymbol{r})$ is the centripetal force, which is also perpendicular to both $\boldsymbol{\Omega}$ and $\boldsymbol{V}$ but is directed toward the axis of rotation. $\boldsymbol{T}$ is the viscous stress tensor and ρ_{nf} is the density of nanofluid. In component form it can be written as

$$\frac{\partial u}{\partial x}+\frac{\partial v}{\partial y}=0, \tag{2}$$

$$\rho_{nf}\left(u\frac{\partial u}{\partial x}+v\frac{\partial u}{\partial y}+2\Omega\, w\right)=-\frac{\partial p^*}{\partial x}+\mu_{nf}\left(\frac{\partial^2 u}{\partial x^2}+\frac{\partial^2 u}{\partial y^2}\right), \tag{3}$$

$$\rho_{nf}\left(u\frac{\partial v}{\partial x}+v\frac{\partial v}{\partial y}\right)=-\frac{\partial p^*}{\partial y}+\mu_{nf}\left(\frac{\partial^2 v}{\partial x^2}+\frac{\partial^2 v}{\partial y^2}\right), \tag{4}$$

$$\rho_{nf}\left(u\frac{\partial w}{\partial x}+v\frac{\partial w}{\partial y}-2\Omega u\right)=\mu_{nf}\left(\frac{\partial^2 w}{\partial x^2}+\frac{\partial^2 w}{\partial y^2}\right), \tag{5}$$

Where $p^*=p-\frac{\Omega^2x^2}{2}$ is the modified pressure and μ_{nf} is the effective dynamic viscosity of nanofluid, the absence of $\frac{\partial p^*}{\partial z}$ depicts the net cross flow along z-axis. The heat transfer phenomenon can be expressed mathematically as

$$u\frac{\partial T}{\partial x}+v\frac{\partial T}{\partial y}=\frac{k_{nf}}{(\rho c)_{nf}}\left(\frac{\partial^2 T}{\partial x^2}+\frac{\partial^2 T}{\partial y^2}\right). \tag{6}$$

T denotes the temperature of the fluid. Where $\alpha_{nf}=\frac{k_{nf}}{(\rho c)_{nf}}$ is the thermal diffusivity of the nanofluid i.e. the ratio of effective heat capacity $(\rho c)_{nf}$ of the nanofluid to effective thermal conductivity k_{nf} of nanofluid. The effective density of the nanofluid is given by

$$\rho_{nf}=(1-\phi)\rho_f+\phi\rho_{CNT}, \tag{7}$$

The heat capacity of the nanofluid and the effective dynamic viscosity μ_{nf} are defined as

$$(\rho c)_{nf}=(1-\phi)(\rho c)_f+\phi(\rho c)_{CNT},\ \mu_{nf}=\frac{\mu_f}{(1-\phi)^{2.5}}, \tag{8}$$

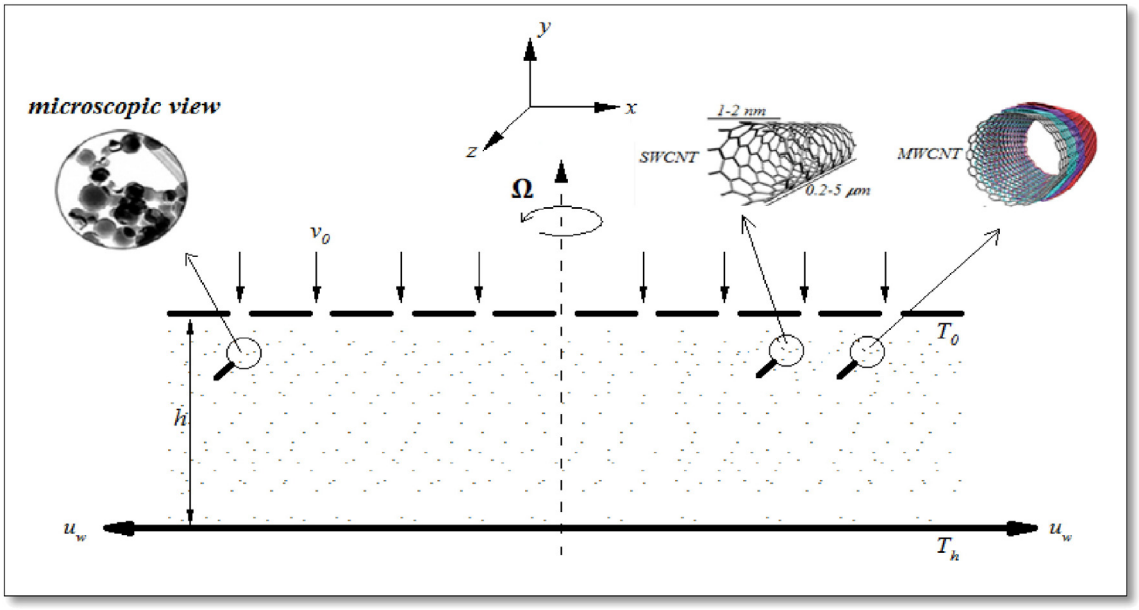

Fig. 1. Geometry of the problem.

$$k_{nf} = k_f \left(\frac{1-\phi + 2\phi \frac{k_{CNT}}{k_{CNT-k_f}} \ln\left(\frac{k_{CNT+k_f}}{2k_f}\right)}{1-\phi + 2\phi \frac{k_f}{k_{CNT-k_f}} \ln\left(\frac{k_{CNT+k_f}}{2k_f}\right)} \right). \tag{9}$$

Where, μ_f is the dynamic viscosity of base fluid, k_{nf} is the thermal conductivity and ϕ is the nanoparticle volumetric fraction. The subscripts *CNT*, *nf* and *f* are used for carbon nanotubes, nanofluid and base fluid respectively. Since the upper wall is porous so the y-component of velocity at the upper wall is not zero (constant for uniform suction/injection case). To develop the net temperature gradient across the fluid, upper wall is kept at lower temperature T_0 and the lower wall at higher temperature T_h i.e. $T_h > T_0$. The boundary constraints for the system can be defined as

$$u = U_w = ax, v = 0, w = 0, T = T_h \text{ at } y = 0, \tag{10}$$

$$u = 0, v = -V_0, w = 0, T = T_0 \text{ at } y = h. \tag{11}$$

In the above V_0 is the uniform suction ($V_0>0$)/injection ($V_0<0$) velocity at the upper wall. Introducing the following similarity transformations and eliminating the pressure gradient

$$u = axf'(\eta), v = -ahf(\eta), w = axg(\eta), \tag{12}$$

$$\theta(\eta) = \frac{T-T_0}{T_h-T_0}, \eta = \frac{y}{h}. \tag{13}$$

The non-dimensional system of equation is given by

$$f^{iv} - A_1\epsilon_1\left(f'f'' - ff'''\right) - 2A_2\,\epsilon_1 g' = 0, \tag{14}$$

$$g'' - A_1\epsilon_1(gf' - fg') + 2A_2\,\epsilon_1 f' = 0, \tag{15}$$

$$\theta'' + Pr\epsilon_2 \frac{A_1}{\epsilon_3} f\theta' = 0, \tag{16}$$

subject to the following non-dimensional boundary conditions

$$\left.\begin{array}{l} f(0) = 0, f'(0) = 1, g(0) = 0, \theta(0) = 1 \\ f(1) = S, f'(1) = 0, g(1) = 0, \theta(1) = 0 \end{array}\right\}. \tag{17}$$

In the above equations prime denotes derivative with respect to "η". $S = V_0/ah$ is the suction/injection parameter. The non-dimensional system of equation contains the following parameters

$$A_1 = \frac{ah^2}{\nu_f}\,(Reynold's\ number), A_2 = \frac{\Omega h^2}{\nu_f}\ (rotation\ parameter), \tag{18}$$

$$\epsilon_3 = \frac{k_{nf}}{k_f} = \frac{1-\phi + 2\phi \frac{k_{CNT}}{k_{CNT-k_f}} \ln\frac{k_{CNT}+k_f}{2k_f}}{1-\phi + 2\phi \frac{k_f}{k_{CNT-k_f}} \ln\frac{k_{CNT}+k_f}{2k_f}}, (thermal\ conductivities\ ratio\ ) \tag{19}$$

$$\epsilon_1 = \left[(1-\phi) + \phi\frac{\rho_{CNT}}{\rho_f}\right](1-\phi)^{2.5}, \tag{20}$$

$$\epsilon_1 = \left[(1-\phi) + \phi\frac{(\rho c_p)_{CNT}}{(\rho c_p)_f}\right]. \tag{21}$$

The important physical parameter skin friction coefficient and local Nusselt number are defined as

$$c_f = \frac{\tau_w}{\frac{\rho_{nf}U_w^2}{2}}, \tag{22}$$

$$Nu_x = \frac{xq_w}{k_{nf}(T_w - T_\infty)} \tag{23}$$

where $\tau_w = \mu_{nf}\left(\frac{\partial u}{\partial y}\right)_{y=0}$ is the shear stress at wall and $q_w = -k_{nf}\left(\frac{\partial T}{\partial y}\right)_{y=0}$ is the heat flux at wall. Eq. (22) is written in terms of nanofluid properties as defined in the recent article of Choi et al. [31]. He has shown that the controversies in the experimental and numerical studies [32–34] were owing to the definition of Nusselt number in terms of base fluid properties rather than nanofluid properties. Also the trend prediction of Nusselt number by homogenous and Boungiorono model is similar if

it is defined in terms of nanofluid properties. Keeping this fact in mind we also defined the skin friction in terms of nanofluid properties and found that it's non-dimensional expression also depends upon the nanoparticles volumetric fraction and density of nanofluid, which is close to the experimental observations that skin friction depends upon the volume percentage of nanoparticles and their density. By means of similarity transformation defined in Eqs. (12) and (13), the resulting form of Eqs. (22) and (23) takes the following form:

$$C_f Re_x^{\frac{1}{2}} = \left.\frac{f''(\eta)}{\left(\frac{1}{(1-\phi)+\phi\frac{\rho_p}{\rho_f}}\right)(1-\phi)^{2.5}}\right|_{\eta=0} , Re_x^{-1/2}Nu_x = -\theta'(\eta)|_{\eta=0} \text{ (lower surface of channel)} \quad (24)$$

$$C_f Re_x^{\frac{1}{2}} = \left.\frac{f''(\eta)}{\left(\frac{1}{(1-\phi)+\phi\frac{\rho_p}{\rho_f}}\right)(1-\phi)^{2.5}}\right|_{\eta=1} , Re_x^{-1/2}Nu_x = -\theta'(\eta)|_{\eta=1} \text{ (upper surface of channel)} \quad (25)$$

Where, $Re_x = \frac{U_w x}{\nu_f}$ is the local Reynold number.

3. Methodology

The above-mentioned coupled differential Eqs. (14) to (16) along with the boundary conditions defined in Eq. (17) are tackled through a numerical technique. Since the present mathematical model contains the two point boundary value problem (BVP) so these equations are solved with the help of the Runge–Kutta–Fehlberg (RKF) method. The step size is taken as $\Delta\eta = 0.01$ and the procedure for the RKF method is repeated until we get the asymptotically convergent results within a tolerance level of 10^{-6}. All these working schemes are assimilated in the computational software MATLAB.

4. Results and discussion

In order to analyze the flow and heat transfer behavior, results are plotted in Figs. 2–5, describing the variation in the velocities ($f'(\eta)$ and $g(\eta)$) and temperature functions $\theta(\eta)$ within the restricted domain, defined in the geometry. Before the analysis of graphical discussion Tables 2 and 3 are constructed for skin friction coefficient and local Nusselt number for various values of emerging parameters. These results are plotted against the nanoparticle volume fraction ϕ, suction/injection parameter s A_1 and rotation parameter A_2. Fig. 2(a–c) provides the comparison between the single wall (SWCNT) and multiple wall carbon nanotubes (MWCNT) with the various values of nanoparticle volume fraction ϕ. Although in Fig. 2(a) there is a very slight variation in the velocity $f'(\eta)$ for increasing values of nanoparticle volume fraction ϕ. But it can be observed in the inset of Fig. 2(a) that SWCNTs have comparatively low velocity profile as compared to MWCNTs. Fig. 2(b) depicts the variation in $g(\eta)$ with the various values of nanoparticle volume fraction. As we can see, base fluid has comparatively higher velocity distribution along z-direction as compared to the water based CNTs. Moreover it can be observed that water based SWCNTs have comparatively higher velocity profile $g(\eta)$ as compared to the water based MWCNTs. Fig. 2(c) shows the variation of temperature profile against nanoparticle volume fraction ϕ. We can observe in Fig. 2(c), temperature profile increases with respect to nanoparticle volume fraction ϕ, however SWCNTs have almost the same temperature profile when it is compared with the MWCNTs. (See Table 1.)

Fig. 3(a) and (b) demonstrates the velocity distribution along the x and w direction, respectively. Fig. 3(a–c)is plotted against the suction/injection parameter s. For each suction and injection case, velocity profile $f'(\eta)$ along the x-direction and $g(\eta)$ along the w-direction increase, respectively. Further it can be observed that, at the mean position of the channel, variation in the velocities is more significant as compared to the vicinity of the lower and upper plate of the channel. They also depict that the peak value of the velocity slightly shifts toward the lower wall for positive s while for negative s, it slightly shifts toward the upper plate. Fig. 3(c) depicts the variation of temperature profile with the various values of suction/injection parameter s. It can be determined that increasing values of suction/injection parameter s resist the temperature distribution and hence it gives the decrease in the temperature profile. Fig. 4(a–c)is plotted for $f'(\eta)$, $g(\eta)$ and $\theta(\eta)$ with the various values of A_1. Through plotted results in Fig. 4(a), the parameter A_1 gives two different behaviors for velocity profile $f'(\eta)$. One can see that at the mean position of the channel velocity distribution swapping its behavior from increasing to decreasing with the various values of A_1. This effect is primarily due to stretching of the lower plate. However in Fig. 4(b), the velocity distribution $g(\eta)$ shows the uniform decreasing

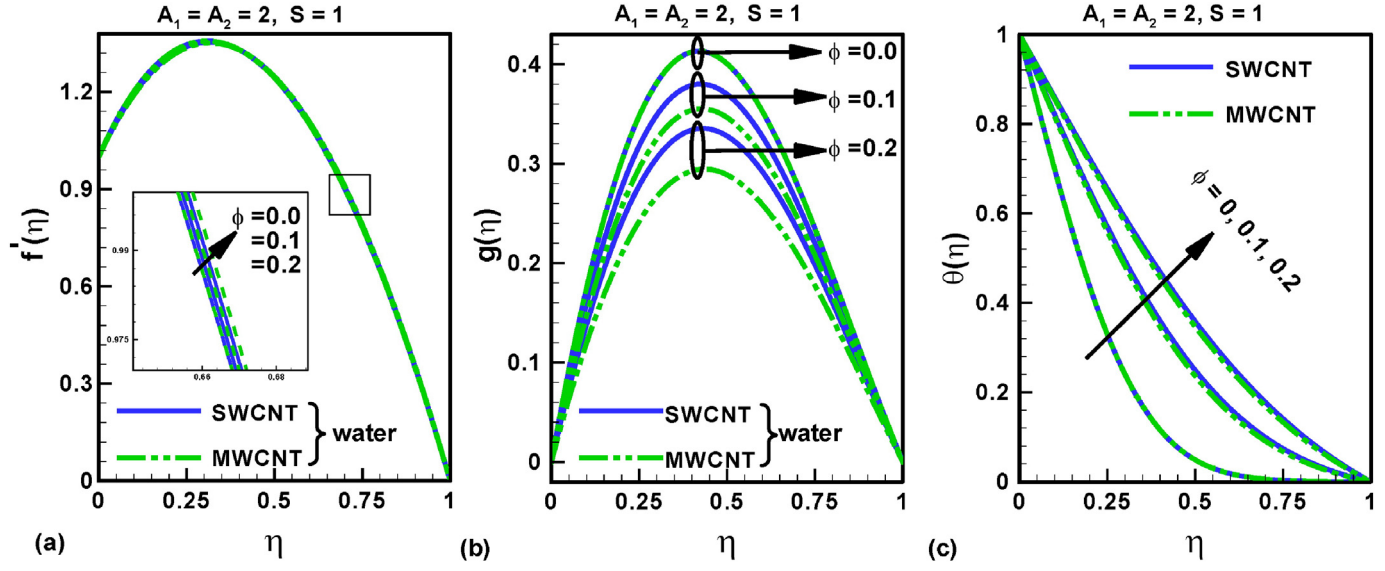

Fig. 2. Variation of (a) $f'(\eta)$ (b) $g(\eta)$ (c) $\theta(\eta)$ with respect to various values of ϕ.

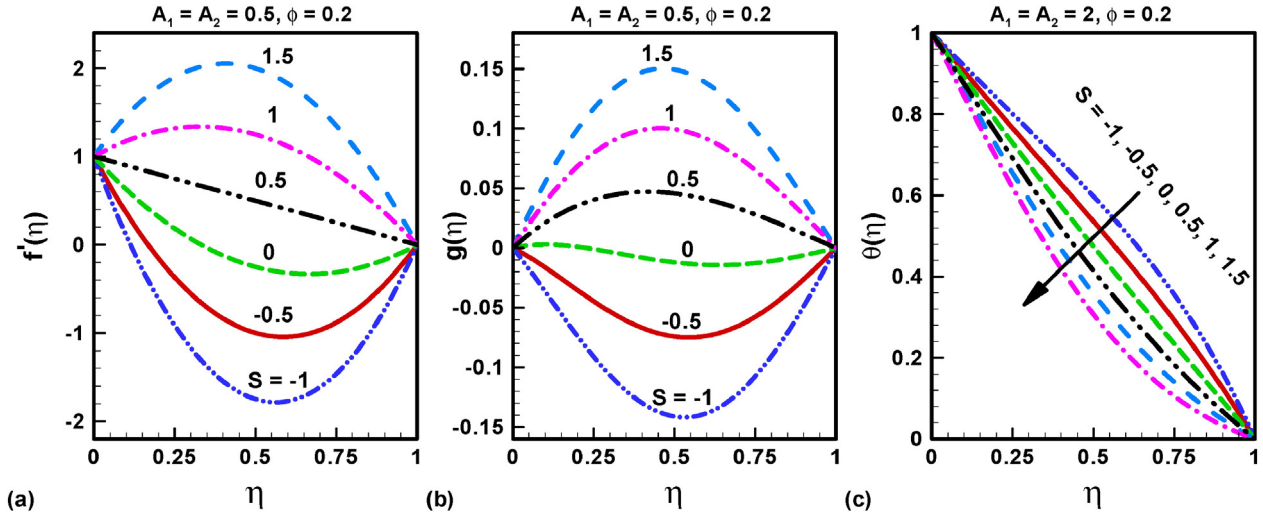

Fig. 3. Variation of (a) $f'(\eta)$ (b) $g(\eta)$ (c) $\theta(\eta)$ with respect to various values of S.

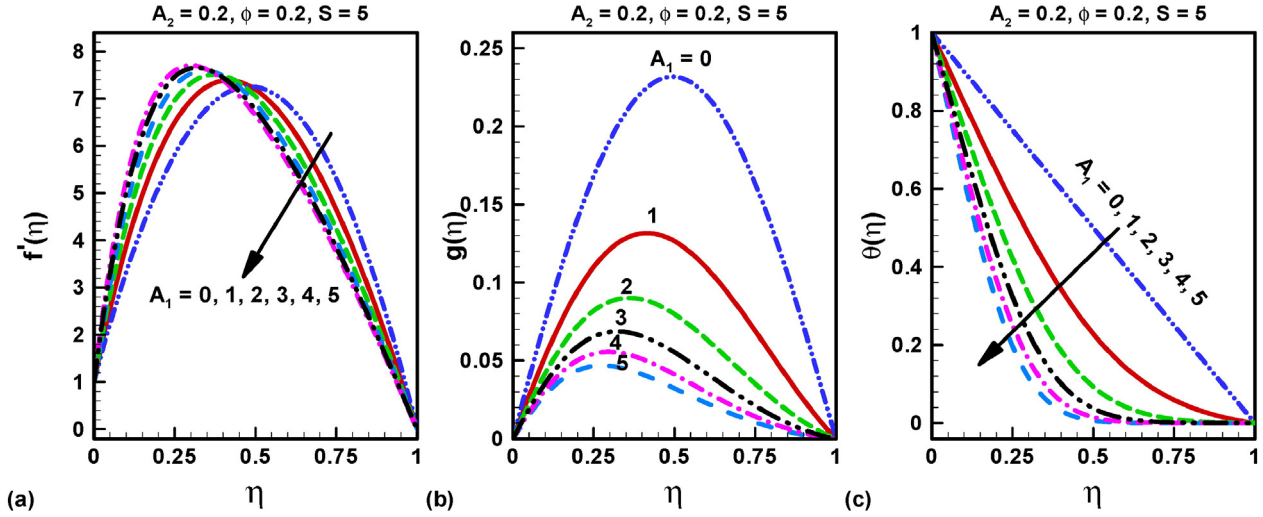

Fig. 4. Variation of (a) $f'(\eta)$ (b) $g(\eta)$ (c) $\theta(\eta)$ with respect to various values of A_1.

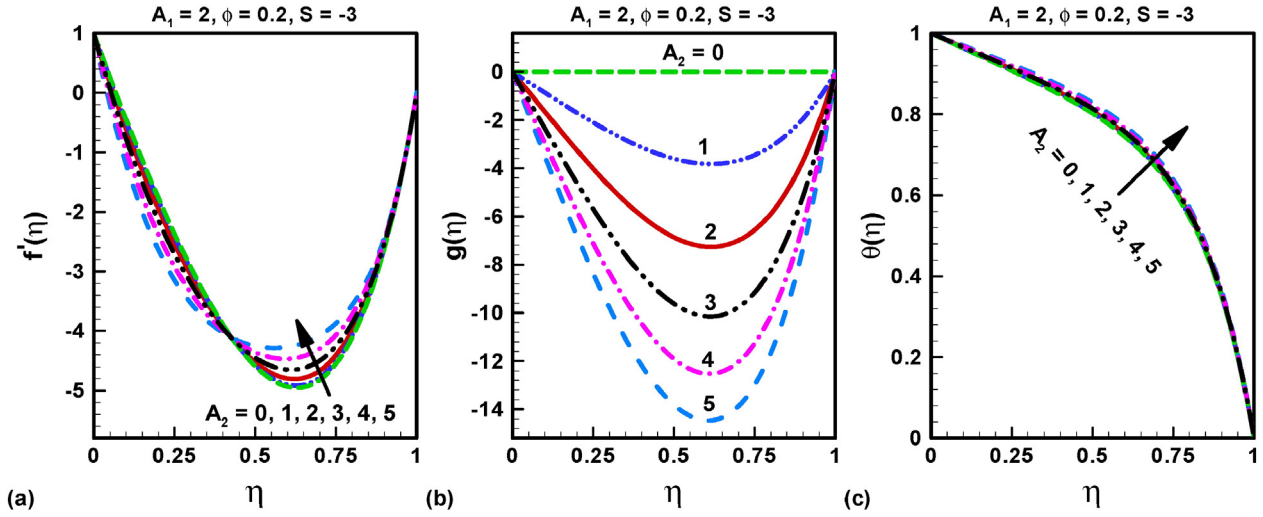

Fig. 5. Variation of (a) $f'(\eta)$ (b) $g(\eta)$ (c) $\theta(\eta)$ with respect to various values of A_2.

Table 1
Thermophysical properties of different base fluids and CNTs [15].

Physical properties	Base fluids	Nanoparticles	
	Water	SWCNT	MWCNT
ρ (kg/m^3)	997	2600	1600
Cp (J/kg K)	4179	425	796
k (W/m K)	0.613	6600	3000
Pr	6.2		

behavior with respect to higher values of A_1. For the case of static lower plate the velocity profile is completely symmetric about the mean position of the channel as the value of A_1 increases the peak value of velocity shifts toward the lower plate. The decreasing behavior of the temperature profile $\theta(\eta)$ has attained with increasing values of A_1 (see Fig. 4(c)). When A_1 is zero i.e. the lower plate is at rest. The temperature profile shows a linear decreasing behavior from maximum value 1 to the minimum value zero. For other values of A_1 it shows the nonlinear decreasing behavior.

Fig. 5 carries the variation in the velocities ($f'(\eta)$ and $g'(\eta)$) and temperature profile $\theta(\eta)$ with respect to the various values of A_2. In Fig. 5(a), it is found that variation in the velocity profile $f'(\eta)$ within the restricted domain gives dual nature behavior. It can be observed that the velocity profile $f'(\eta)$ gives decreasing behavior with the various values of rotating parameter A_2 within the region $0 \le \eta \le 0.5$, however these results are quite opposite within the domain $0.5 \le \eta \le 1$. The rotating parameter A_2 gives the more dominant variation for velocity profile at the upper half of the channel. In Fig. 5(b), one can see that in the absence of rotating parameter ($A_2 = 0$), $z-$ component of the velocity, so in the absence of rotation this problem reduces to the steady two-dimensional flow in a channel. However, velocity distribution $g(\eta)$ gives the decreasing behavior with the increasing values of A_2. Further it can be seen that at the mean position of the channel disturbance in the velocity is higher as compared to the lower and upper surface of the channel. Fig. 5(c) shows the increasing behavior in the temperature profile with respect to the rotating parameter A_2.

To analyze the skin friction of the fluid at the lower surface of the channel, results are plotted against each physical parameter for both SWCNTs and MWCNTs. In Fig. 6(a), skin friction coefficient is plotted for both suction/injection parameter s and nanoparticle volume fraction ϕ. It is noticed that the absolute values of skin friction coefficient increase with the increase in nanoparticle volumetric fraction irrespective of the case of suction or injection. Also MWCNTs have higher skin friction coefficient as compared to the SWCNTs irrespective of the values of the pertinent parameters. Fig. 6(b) and (c) depicts the variation of skin friction w.r.t. rotating parameter, skin friction coefficient gives the same increasing behavior. Fig. 7(a–c) shows the variation of skin friction coefficient at the upper wall due to the rotation and forced convection at the lower wall. Overall skin friction shows increase with respect to nanoparticle volumetric fraction irrespective of the other pertinent parameters. The skin friction behavior at the upper wall is similar to that of the lower wall for suction/injection and rotation parameter. For A_1 skin friction at the upper wall shows the decreasing behavior.

Fig. 8(a–c) describes the influence of physical parameter on local Nusselt number. In Fig. 8(a), it is found that for $s = 0$ and $s = 1$, there is a decreasing behavior in the heat transfer w.r.t. increasing values of nanoparticle volume friction ϕ. However, $s = -1$ behavior for local Nusselt number is quite opposite and increasing with respect to various values of nanoparticle volume friction ϕ. Influence of rotation parameters A_1 and A_2 and nanoparticle volume friction ϕ on local Nusselt number is plotted in Fig. 8(b) and (c). It is observed that, there is rapid rise in the local Nusselt number with the simultaneous increase in the rotation parameter and nanoparticle volume friction. Furthermore it is found that water based MWCNTs pound high heat transfer rate as compared to MWCNTs. Fig. 9(a–c) shows the variation of Nusselt number at upper wall against the nanoparticle volumetric fraction. Fig. 9(a–b)

Table 2
Numerical values of skin friction coefficient against the various values of emerging parameters.

$S\downarrow$	$\phi\downarrow$	$C_f Re_x^{1/2}$ at $\eta=0$				$C_f Re_x^{1/2}$ at $\eta=1$			
		$A_2=0$		$A_2=1$		$A_2=0$		$A_2=1$	
		$A_1=0.5$	$A_1=1$	$A_1=0.5$	$A_1=1$	$A_1=0.5$	$A_1=1$	$A_1=0.5$	$A_1=1$
−1	0.0	−9.73485	−9.46810	−9.79701	−9.54155	8.38630	8.80893	8.43150	8.85752
	0.1	−10.94616	−10.67966	−11.00066	−10.74281	9.35337	9.76990	9.39338	9.81257
	0.2	−12.95422	−12.68803	−12.99946	−12.73922	10.95734	11.36633	10.99095	11.40183
0	0.0	−4.04282	−4.08556	−4.05316	−4.09595	1.97639	1.95318	1.97585	1.95289
	0.1	−4.52731	−4.57007	−4.53654	−4.57933	2.21861	2.19534	2.21811	2.19503
	0.2	−5.33049	−5.37326	−5.33832	−5.38111	2.62017	2.59682	2.61972	2.59651
1	0.0	2.10694	2.21327	2.13398	2.23565	−3.88037	−3.77309	−3.92117	−3.81099
	0.1	2.34921	2.45567	2.37382	2.47647	−4.36417	−4.25497	−4.40085	−4.28935
	0.2	2.75083	2.85743	2.77224	2.87600	−5.16647	−5.05484	−5.19788	−5.08459

Table 3
Numerical values of local Nusselt number against the various values of emerging parameter.

$S\downarrow$	$\phi\downarrow$	$Re_x^{-1/2} Nu_x$ at $\eta=0$				$Re_x^{-1/2} Nu_x$ at $\eta=1$			
		$A_2=0$		$A_2=1$		$A_2=0$		$A_2=1$	
		$A_1=0.5$	$A_1=1$	$A_1=0.5$	$A_1=1$	$A_1=0.5$	$A_1=1$	$A_1=0.5$	$A_1=1$
−1	0.0	0.67952	0.39074	0.67911	0.39001	2.43038	4.82218	2.43055	4.82296
	0.1	0.90091	0.80244	0.90078	0.80213	1.35280	1.79110	1.35284	1.79126
	0.2	0.95033	0.90141	0.95029	0.90130	1.16777	1.35524	1.16778	1.35528
0	0.0	1.16185	1.33661	1.16161	1.33610	0.89872	0.80217	0.89889	0.80249
	0.1	1.04993	1.10094	1.04987	1.10082	0.96741	0.93550	0.96746	0.93559
	0.2	1.02508	1.05036	1.02506	1.05032	0.98347	0.96718	0.98349	0.96721
1	0.0	1.62894	2.19513	1.62886	2.19498	0.26551	0.05769	0.26564	0.05776
	0.1	1.20111	1.40509	1.20108	1.40500	0.67410	0.44121	0.67418	0.44132
	0.2	1.10112	1.20408	1.10111	1.20405	0.82221	0.67045	0.82224	0.67051

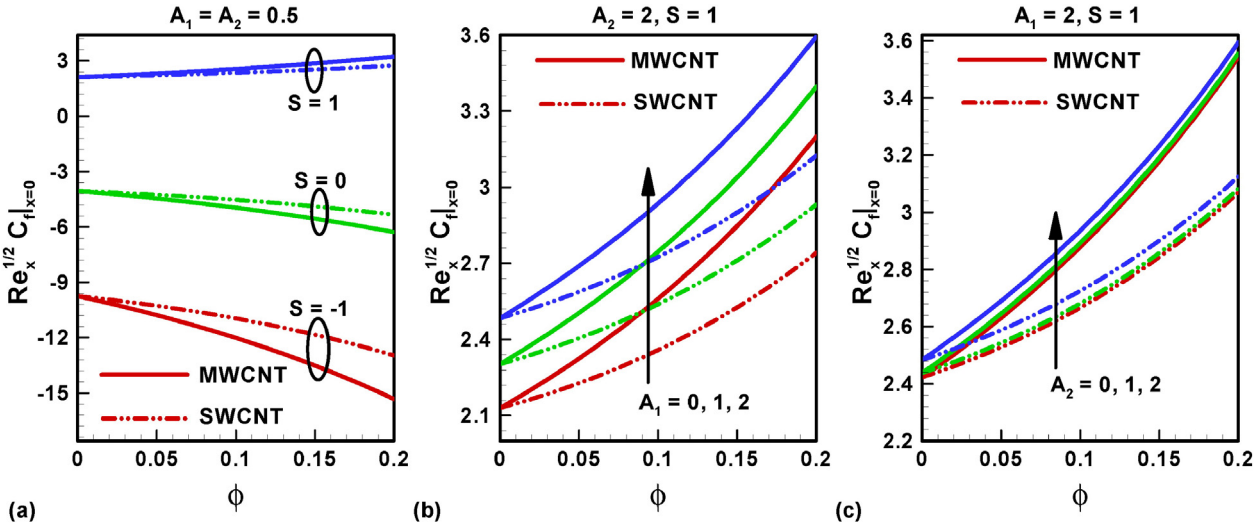

Fig. 6. Variation of skin friction coefficient at $\eta = 0$ for (a) S (b) A_2 (c) A_1.

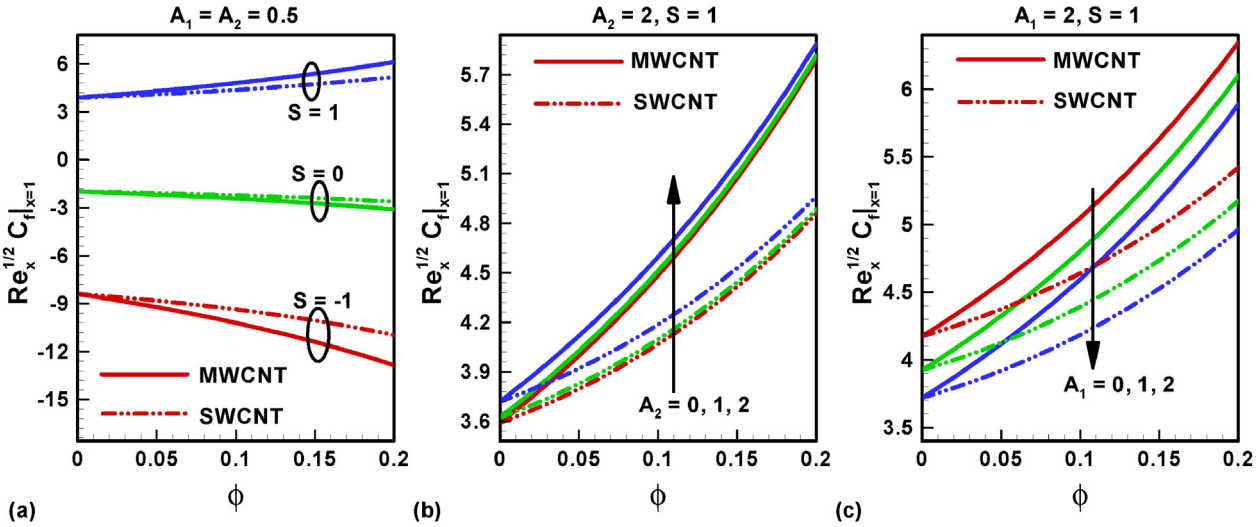

Fig. 7. Variation of skin friction coefficient at $\eta = 1$ for (a) S (b) A_2 (c) A_1.

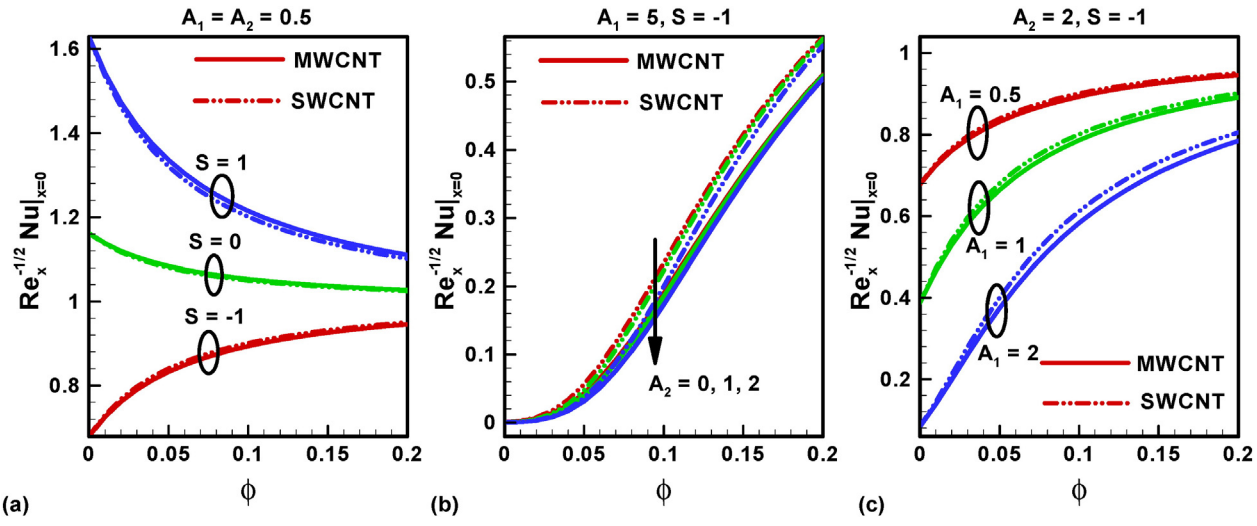

Fig. 8. Variation of local Nusselt number at $\eta = 0$ for (a) S (b) A_2 (c) A_1.

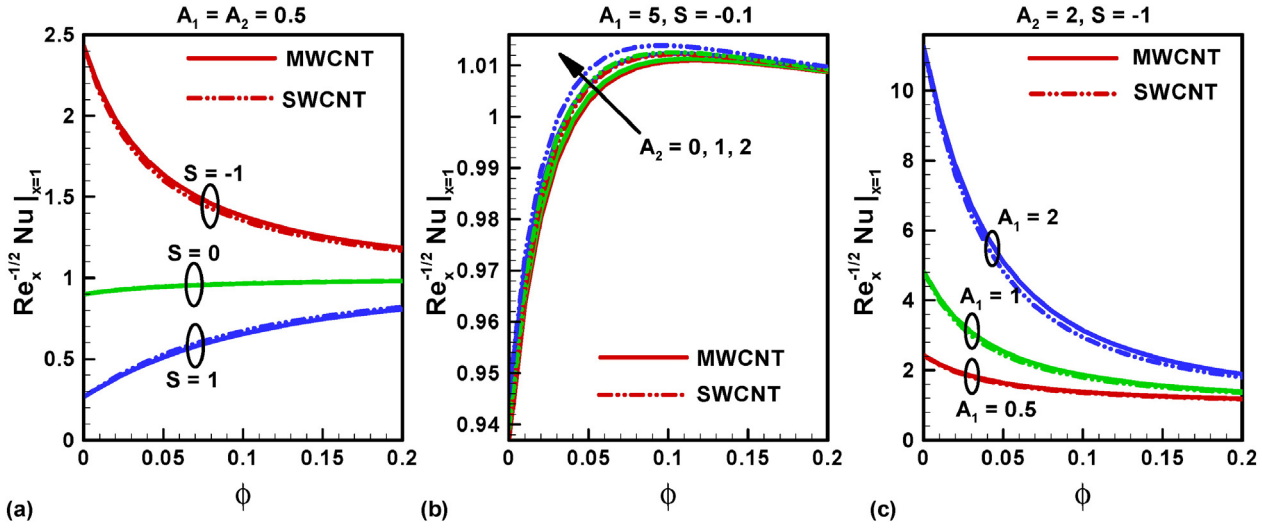

Fig. 9. Variation of local Nusselt number at $\eta = 1$ for (a) S (b) A_2 (c) A_1.

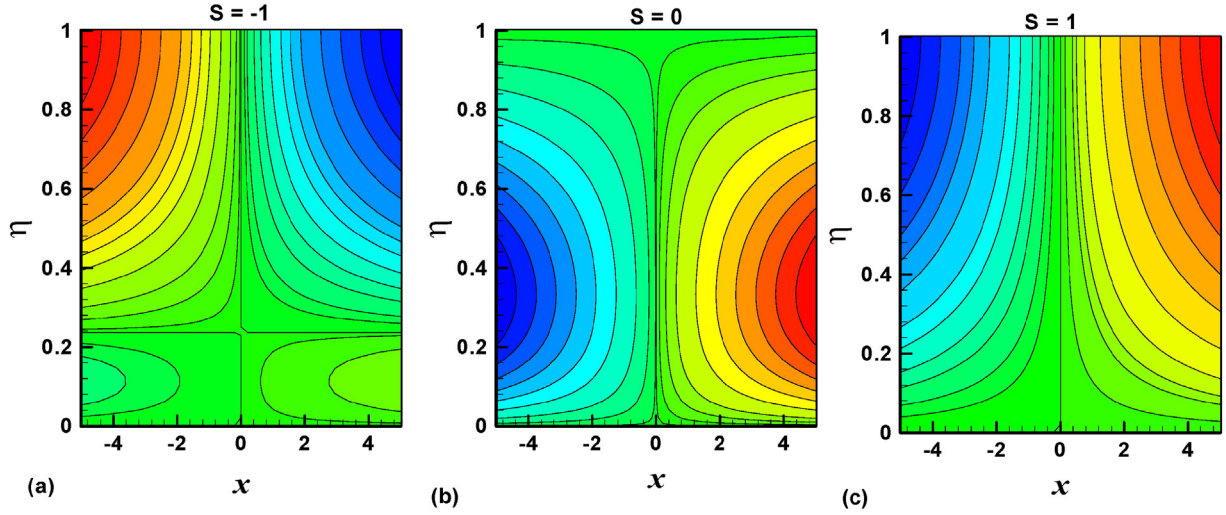

Fig. 10. Variation of stream lines for various values of S.

shows the increase in the Nusselt number at upper wall with the increase in nanoparticle volumetric fraction, suction/injection parameter and rotation parameter. The different behavior comes against A_1. The Nusselt number decreases for both nanoparticle volumetric fraction and A_1. Variations in the stream lines are plotted in Fig. (10) for various values of suction/injection parameter s.

5. Conclusion

Effects of single wall and multiple wall carbon nanotubes have been examined by using the thermos-physical properties of carbon nanotubes for water based nanofluid flow in a rotating frame of system. The flow drag and heat transfer rate has been discussed through plotting the graphs of skin friction and Nusselt number. Incorporation of SWCNTs in this type of flow is better than MWCNTs due to less drag and high rate of heat transfer. This study can be concluded in the following points:

- SWCNTs provide less resistance to the fluid flow as compared to the MWCNTs. Resultantly, SWCNTs have small skin friction coefficient as compared to the MWCNTs.
- Behavior of temperature profile is similar for both SWCNTs and MWCNTs but the SWCNTs have higher Nusselt number against the nanoparticle volumetric fraction as compared to the MWCNTs.
- Suction/injection parameter greatly influences the flow field. Particularly, the position of peak value of velocity is changed according to the value of suction/injection parameter.
- Increase in the rotation parameter causes the increase in the velocity profile and temperature field.
- Increase in rotation parameter causes the drag increase while it decreases the Nusselt number.
- Variation of steam lines depicts the fluid pattern as per suction/injection parameter S.

References

[1] S.U.S. Choi, Enhancing Thermal Conductivity of Fluids with Nanoparticles. The Proceedings of the 1995 ASME International Mechanical Engineering Congress and Exposition. ASME, San Francisco, USA, FED 231/MD 66 1995, pp. 99–105.
[2] H. Masuda, A. Ebata, K. Teramae, N. Hishinuma, Alteration of thermal conductivity and viscosity of liquid by dispersing ultrafine particles, Netsu Bussei 7 (4) (1993) 227–233.

[3] B.C. Pak, I. Cho, Hydromagnetic and heat transfer study of dispersed fluids with submicron metallic oxide particles, Exp. Heat Transfer 11 (1998) 151.
[4] L. Godson, B. Raja, D. Mohan Lal, S. Wongwises, Experimental investigation on the thermal conductivity and viscosity of silver-deionized water nanofluid, Exp. Heat Transfer 23 (4) (2010) 317–332.
[5] N.S. Akbar, Biomathematical analysis of carbon nanotubes due to ciliary motion, Int. J. Biomath. 8 (2) (2015) 1550023.
[6] R. Ellahi, A. Riaz, S. Nadeem, A theoretical study of Prandtl nanofluid in a rectangular duct through peristaltic transport, Appl. Nanosci. 4 (6) (2014) 753–760.
[7] J. Buongiorno, Convective transport in nanofluids, J. Heat Transf. 128 (2006) 240–250.
[8] X. Huang, X. Teng, D. Chen, F. Tang, J. He, The effect of the shape of mesoporous silica nanoparticles on cellular uptake and cell function, Biomaterials 31 (3) (2010) 438–448.
[9] S. Ferrouillat, A. Bontemps, O. Poncelet, O. Soriano, J.A. Gruss, Influence of nanoparticle shape factor on convective heat transfer of water-based ZnO nanofluids. Performance evaluation criterion, Int. J. Mech. Ind. Eng. 1 (2) (2011) 1–13.
[10] A. Albanese, P.S. Tang, W.C. Chan, The effect of nanoparticle size, shape, and surface chemistry on biological systems, Annu. Rev. Biomed. Eng. 14 (2012) 1–16.
[11] M.M. Elias, M. Miqdad, I.M. Mahbubul, R. Saidur, M. Kamalisarvestani, M.R. Sohel, N.A. Arif Hepbasli, M.A. Rahim, Amalina, Effect of nanoparticle shape on the heat transfer and thermodynamic performance of a shell and tube heat exchanger, Int. Commun. Heat Mass Transfer 44 (2013) 93–99.
[12] S.M. Vanaki, H.A. Mohammed, A. Abdollahi, M.A. Wahid, Effect of nanoparticle shapes on the heat transfer enhancement in a wavy channel with different phase shifts, J. Mol. Liq. 196 (2014) 32–42.
[13] L. Jeong, Y. Chengguo, J. Kwon, S.H.K. Lee, R. Yun, Particle shape effect on the viscosity and thermal conductivity of ZnO nanofluids, Int. J. Refrig. 36 (8) (2013) 2233–2241.
[14] E.V. Timofeeva, J.L. Routbort, D. Singh, Particle shape effects on thermophysical properties of alumina nanofluids, J. Appl. Phys. 106 (2009) 014304.
[15] R.U. Haq, S. Nadeem, Z.H. Khan, N.F.M. Noor, Convective heat transfer in MHD slip flow over a stretching surface in the presence of carbon nanotubes, Phys. B Condens. Matter 457 (2015) 40–47.
[16] R.U. Haq, Z.H. Khan, W.A. Khan, Thermophysical effects of carbon nanotubes on MHD flow over a stretching surface, Phys. E: Low-dimens. Sys. Nanostruct. 63 (2014) 215–222.
[17] B.C. Sakiadis, Boundary layer behavior on continuous solid flat surfaces, Am. Inst. Chem. Eng. J. (1961) 726–728.
[18] F.K. Tsou, E.M. Sparrow, R.J. Goldstein, Flow and heat transfer in the boundary layer on a continuous moving surface, Int. J. Heat Mass Transf. 10 (1967) 219.
[19] L.E. Erickson, L.T. Fan, V.G. Fox, Heat and mass transfer in the laminar boundary layer flow of a moving flat surface with constant surface velocity and temperature focusing on the effects of suction/injection, Ind. Eng. Chem. Res. 5 (1966) 19.
[20] S. Nadeem, S.T. Hussain, Flow and heat transfer analysis of Williamson nanofluid, Appl. Nanosci. 4 (2014) 1005–1012.
[21] S.T. Hussain, S. Nadeem, R.U. Haq, Model-based analysis of micropolar nanofluid flow over a stretching surface, Eur. Phys. J. Plus 129 (2014) 161.
[22] R. Ellahi, M. Hassan, A. Zeeshan, Shape effects of nanosize particles in Cu–H_20 nanofluid on entropy generation, Int. J. Heat Mass Transf. 81 (2015) 449–456.
[23] M. Sheikholeslami, D.D. Ganji, M.Y. Javed, R. Ellahi, Effect of thermal radiation on nanofluid flow and heat transfer using two phase model, J. Magn. Magn. Mater. 374 (2015) 36–43.
[24] S. Rashidi, M. Dehghan, R. Ellahi, M. Riaz, M.T. Jamalabad, Study of stream wise transverse magnetic fluid flow with heat transfer around a porous obstacle, J. Magn. Magn. Mater. 378 (2015) 128–137.
[25] N.S. Akbar, M. Raza, R. Ellahi, Influence of heat generation and heat flux in peristalsis with interaction of nanoparticles, Eur. Phys. J. – Plus 129 (2014) 185.
[26] M. Sheikholeslami, R. Ellahi, M. Hassan, S. Soleimani, A study of natural convection heat transfer in a nanofluid filled enclosure with elliptic inner cylinder, Int. J. Numer. Methods Heat Fluid Flow 24 (8) (2014) 1906–1927.
[27] M. Sheikholeslami, R. Ellahi, H.R. Ashorynejad, G. Domairry, T. Hayat, Effects of heat transfer in flow of nanofluids over a permeable stretching wall in a porous medium, Comput. Theor. Nanosci. 11 (2) (2014) 486–496.
[28] M. Sheikholeslami, M.G. Bandpy, R. Ellahi, A. Zeeshan, Simulation of CuO–water nanofluid flow and convective heat transfer considering Lorentz forces, J. Magn. Magn. Mater. 369 (2014) 69–80.
[29] N.S. Akbar, M. Raza, R. Ellahi, Interaction of nano particles for the peristaltic flow in an asymmetric channel with the induced magnetic field, Eur. Phys. J. – Plus 129 (2014) 155–167.
[30] R.U. Haq, S. Nadeem, Z.H. Khan, N.F.M. Noor, MHD squeezed flow of water functionalized metallic nanoparticles over a sensor surface, Phys. E: Low-dimens. Syst. Nanostruct. 73 (2015) 45–53.
[31] A.K. Borkakoti, A. Bharali, Hydromagnetic flow and heat transfer between two horizontal plates, the lower plate being a stretching sheet, Q. Appl. Math. 40 (4) (1982) 461–467.
[32] S. Hussnain, A. Mehmood, A. Ali, Three-dimensional channel flow of second grade fluid in rotating frame, Appl. Math. Mech. 33 (3) (2012) 289–302 (English edition).
[33] K. Vajravelu, B.V.R. Kumar, Analytical and numerical solutions of a coupled nonlinear system arising in a three-dimensional rotating flow, Int. J. Non Linear Mech. 39 (1) (2004) 13–24.
[34] N. Freidoonimehr, B. Rostami, M.M. Rashidi, E. Momoniat, Analytical modelling of three-dimensional squeezing nanofluid flow in a rotating channel on a lower stretching porous wall, Math. Probl. Eng. 692728 (2014).
[35] M. Sheikholeslami, H.R. Ashorynejad, G. Domairry, I. Hashim, Flow and heat transfer of Cu–water nanofluid between a stretching sheet and a porous surface in a rotating system, J. Appl. Math. (2012) 421320.
[36] N.S. Akbar, S.U. Rahman, R. Ellahi, S. Nadeem, Nano fluid flow in tapering stenosed arteries with permeable walls, Int. J. Therm. Sci. 85 (2014) 54–61.
[37] A. Zeeshan, R. Ellahi, M. Hassan, Magnetohydrodynamic flow of water/ethylene glycol based nanofluids with natural convection through porous medium, Eur. Phys. J. Plus 129 (12) (2014) 1–10.
[38] W.A. Khan, R. Culham, R.U. Haq, Heat transfer analysis of MHD water functionalized carbon nanotube flow over a static/moving wedge, J. Nanomater. 13 (2015), 934367http://dx.doi.org/10.1155/2015/934367.
[39] U. Khan, N. Ahmed, S.T. Mohyud-Din, Heat transfer effects on carbon nanotubes suspended nanofluid flow in a channel with non-parallel walls under the effect of velocity slip boundary condition: a numerical study, Neural Comput. & Applic. (2015)http://dx.doi.org/10.1007/s00521-015-2035-4.
[40] S.T. Mohyud-Din, Z.A. Zaidi, U. Khan, N. Ahmed, On heat and mass transfer analysis for the flow of a nanofluid between rotating parallel plates, Aerosp. Sci. Technol. 46 (2015) 514–522.